



The use of Nafion membranes to measure $^2\text{H}/^1\text{H}$ and $^{18}\text{O}/^{16}\text{O}$ isotopic ratios in water

V. López Días^{a,*}, H.Q. Hoang^a, N. Martínez-Carreras^b, F. Barnich^b, T. Wirtz^a, J.J. McDonnell^c, L. Pfister^{b,d}

^a Advanced Instrumentation for Ion Nano-Analytics (AINA), MRT Department, Luxembourg Institute of Science and Technology (LIST), 41 rue du Brill, L-4422 Belvaux, Luxembourg

^b Catchment and Eco-hydrology Research Group (CAT), Environmental Research and Innovation (ERIN), Luxembourg Institute of Science and Technology (LIST), 41 rue du Brill, L-4422 Belvaux, Luxembourg

^c University of Saskatchewan, Global Institute for Water Security, 11 Innovation Boulevard, Saskatoon SK, Canada S7N 3H5

^d University of Luxembourg, Faculty of Science, Communication and Technology, Esch/Alzette, Luxembourg

ARTICLE INFO

Keywords:

Nafion membrane
MI inlet
MIMS inlet
Isotopic fractionation
Water analysis
 $\delta^{18}\text{O}$
 $\delta^2\text{H}$
 $^{18}\text{O}/^{16}\text{O}$ isotopic ratios and $^2\text{H}/^1\text{H}$ isotopic ratios

ABSTRACT

The isotopic composition of water ($^2\text{H}/^1\text{H}$ and $^{18}\text{O}/^{16}\text{O}$) has been widely used in hydrology, ecology, paleoclimatology and forensic science. However, sampling frequency limits many such studies and there is now a clear need for field-portable mass spectrometer and laser-based spectrometer devices to measure water isotopic composition in-situ and at high temporal resolution. Here we explore the use of Nafion membranes as a potential Membrane Introduction (MI) inlet system for high frequency isotope analysis. As yet, the fractionation behaviour of $^2\text{H}/^1\text{H}$ and $^{18}\text{O}/^{16}\text{O}$ isotopic ratios in water transported through Nafion membranes has not been investigated. We quantify this behaviour for water samples with different matrices (organic matter and pollutants) and salinity concentrations across a wide range of isotopic ratios and different membrane thicknesses. Nafion membranes showed no fractionation effects on reported isotope ratios for natural waters. Also no fractionation effects were detected with salinity. Membrane thickness affected slightly the precision and accuracy of the isotopic ratio analysis and our tests showed that thinner Nafion membranes provide better results. However, for samples contaminated with organic matter, the thicker membranes performed better for the $^2\text{H}/^1\text{H}$ isotopic ratio, while for samples contaminated with pollutants, the thicker membranes performed better for the $^{18}\text{O}/^{16}\text{O}$ isotopic ratio. Overall, Nafion membranes appear well suited to MI inlet use and our work suggests that the optimal Nafion membrane thickness is 50–150 μm .

1. Introduction

1.1. Measurement of stable isotopes in water

Stable isotopes of the water molecule ($^2\text{H}/^1\text{H}$ and $^{18}\text{O}/^{16}\text{O}$) are a common tool to study the water cycle. Different waters recharged at different times, in different locations, or that followed different flow-paths are often isotopically distinct [1]. The stable isotopes of water are conservative at ambient temperatures and water retains its distinctive fingerprint until it mixes with waters of different composition [1]. It is during phase changes (e.g. evaporation and condensation), that stable isotopes become enriched in one phase and depleted in the other (i.e. isotopic fractionation). Because of all these properties, the isotopic composition of water is widely used to investigate water processes in

several disciplines. These disciplines include paleoclimatology (e.g. climate reconstruction by the study of ice core water isotopes [2,3], cave ice water isotopes [4] or the temporal ($^{18}\text{O}/^{16}\text{O}$)/temperature relationship [5]), environmental monitoring (e.g. tracking the source and flowpaths in a groundwater system to ensure water quality [6–8], quantification of parasitic discharge in sewers [9]), ecology (e.g. investigation of plant water uptake [10–13], water isotopes as tracers of diet and provenance in the biota of an aquatic ecosystem [14]), forensics (e.g. isotope analyses of cotton fiber to determine its origin by comparing it with the local rain isotopic composition where the cotton plant could grow [15], geographic sourcing of wine [15], dietary and water source information recorded in hair and fingernails to distinguish individuals of different geographic origin, possible sources of mad cow disease, vectors associated with the bird flu, food authenticity [15]) and

* Corresponding author.

E-mail address: veneranda.lopezdias@list.lu (V. López Días).

<https://doi.org/10.1016/j.memsci.2018.11.003>

Received 4 June 2018; Received in revised form 23 October 2018; Accepted 3 November 2018

Available online 05 November 2018

0376-7388/ © 2018 Elsevier B.V. All rights reserved.

hydrology (e.g. tracing water sources, pathways and transit times [1,16,17]).

Variations in the stable isotope ratios of terrestrial water are typically in the parts per thousand range, hence the concentration of each isotope is given by its abundance related to the lighter isotope in the sample, relative to its concentration in an accepted standard (in permil variations (‰)). These ratios are written “ $\delta^2\text{H}$ ” or “ δD ” or “ $^2\text{H}/^1\text{H}$ isotopic ratios” for ^2H and “ $\delta^{18}\text{O}$ ” or “ $^{18}\text{O}/^{16}\text{O}$ isotopic ratios” for ^{18}O (see Eqs. (1) and (2)). $\delta^2\text{H}$ and $\delta^{18}\text{O}$ values are normally reported relative to the Vienna Standard Mean Ocean Water (VSMOW) [18].

$$\delta^2\text{H} = \left[\frac{(^2\text{H}/^1\text{H})_{\text{sample}}}{(^2\text{H}/^1\text{H})_{\text{standard}}} - 1 \right] \times 1000 \quad (1)$$

$$\delta^{18}\text{O} = \left[\frac{(^{18}\text{O}/^{16}\text{O})_{\text{sample}}}{(^{18}\text{O}/^{16}\text{O})_{\text{standard}}} - 1 \right] \times 1000 \quad (2)$$

Stable isotope composition is measured in the laboratory using laser absorption spectrometry techniques, such as the Off-Axis Integrated Cavity Output Spectroscopy (OA-ICOS) and the Cavity Ring-Down Spectroscopy (CRDS). These techniques rely on the Beer-Lambert's law to relate the absorption of laser light when passing through a vaporized water sample to its isotopic composition. Typically, water isotopic laboratories use automatic injectors to transfer liquid water into a heater, which vaporises liquid water before introducing the water vapour into the laser-based spectrometer. However, automatic injectors and heaters are not designed for field conditions and therefore past and ongoing research targets the development of field deployable instruments that allow in-situ measurements of isotopic ratios in water at high frequency and for long periods [19,20]. Hence, reducing the time needed for sample preservation and transport are important research areas. But most pressing of all though is the need to improve sample frequency. Studies in all fields are now limited by sample frequency issues [19] and alternatives to the use of traditional automatic injectors are desperately needed.

1.2. Membrane introduction inlet system

A membrane introduction (MI) inlet system is an advantageous alternative to automatic injectors, as this technique is characterized by short response times, high sensitivity and selectivity, simplicity and absence of sample preparation, which enable direct continuous and on-line monitoring (in-situ/in-vivo) of complex samples. The most common instrument coupled with MI inlet systems is in fact the mass spectrometer (membrane introduction mass spectrometry (MIMS) technique). However, MI inlet systems can be coupled with other instruments, such as laser-based spectrometers [21], ion mobility spectrometers [22] and flame ionization detectors [23].

MIMS was first used in 1963 by Hoch and Kok [24] for direct introduction of dissolved gases into a mass spectrometer. The membrane plays an essential role, as it is the only barrier between the sample stream and the mass spectrometer. The properties of the membrane will determine which analytes are eventually transferred from the sample matrix to the mass spectrometer, therefore making the technique very selective. The analytes pass through the membrane by the pervaporation process in homogenous membranes. The molecules are first dissolved in the upstream surface of the membrane, then diffused through the membrane, and finally desorbed in the downstream part of the membrane, entering the spectrometer. The selectivity and the pervaporation depend not only on the thermodynamic partitioning between the matrix (which contains the analytes) and the membrane material, but also on the differential diffusivity through the membrane [25]. The membrane can also extract and pre-concentrate analytes, achieving higher sensitivity and avoiding sample preparation. The sensitivity of the membrane depends on the permeability of the analyte through the membrane [26]. The transport through the membrane follows Fick's

diffusion law and depends on membrane intrinsic molecular properties, such as the diffusion coefficient and the relative solubility of analytes in the sample versus the solubility in the membrane. The steady-state permeation flux (Fss) is described in Eq. (3) [26,27]. Where A is the membrane surface in contact with the sample matrix, D is the analyte's diffusivity, K is the partition coefficient of the analyte between the matrix and the membrane, C_s is the concentration of the analyte in the matrix, and I is the membrane thickness.

$$FSS \propto \frac{A \times D \times K \times C_s}{I} \quad (3)$$

Nafion membranes have been mostly used for polymer electrolyte membrane (PEM) fuel cells, which are promising energy conversion devices, and for a variety of electrochemical techniques. However, other membranes have been widely used in MIMS. For instance, the most currently used ones are the polydimethylsiloxane (PDMS) membranes, which are robust and efficient for extraction, pre-concentration and transfer of small hydrophobic analytes from several sample matrices [26]. Well known applications using MIMS with PDMS membranes include the analysis of Volatile and Semivolatile Organic Compounds (VOCs and SVOCs) [28–37], Polyaromatic Hydrocarbons (PAHs), estrogenic compounds and pesticides [35,36] and greenhouse gases [37,38]. Polypropylene (PP), Polyethersulfone (PES), polytetrafluoroethylene (PTFE) and nylon membranes are also used in MIMS for homeland security and forensic applications [39]. Nafion membranes were discovered in the late 1960s [40]. In this context, several authors have investigated properties of Nafion membranes, such as water diffusivity, interfacial mass transport, volume available for transport, water sorption, desorption and transport [41–51]. These membranes are cation exchange membranes, which consist of a tetrafluoroethylene (teflon) hydrophobic backbone with a layer of perfluorovinyl ether groups terminated in hydrophilic sulphonated groups within the polymer. Water sorption can swell and restructure the hydrophilic domains, creating a hydrophilic channel through the hydrophobic backbone. This channel allows transporting the protons and diffusing the water through the membrane, as well as controlling the diffusion coefficient [41,52]. This gives Nafion membranes unique properties, such as high permeability to ions and polar/hydroxylated species, high chemical and electrochemical stability, good mechanical strength, high ionic conductivity and good electrical insulation [53]. Such properties qualify Nafion membranes as MI inlet systems coupled to laser and mass spectrometers for water analyses.

When using the MI inlet system, the matrix containing the analytes is in direct contact with the upper stream of the membrane during the pervaporation process. The analytes are then removed from the downstream part of the membrane in the vapour state and at lower pressure. The water transport through a Nafion membrane at low water content is driven mainly by the diffusion of water near the acid functionalized polymer surfaces in the pores. At high water content, the transport occurs via hydraulic permeation in the pores [54]. However, in the case of pervaporation, hydraulic permeation is negligible as the liquid water activity is small [50]. Hence, the mass transfer of analytes through the membrane is driven by the gradient in the chemical potential. This gradient is due to the difference in partial pressures of the analytes when moving through the membrane - created when using a vacuum pump system to reduce the overall pressure on the downstream part of the membrane [55]. This results in the transport of water through the membrane. The transportation rate decreases with time because the water vapour accumulates in the downstream part of the membrane. The steady state - described in terms of pressure (or number of water molecules) - at the downstream part of the membrane is reached once the transportation rate through the membrane is equivalent to the removal rate of the water vapour from the downstream part, either by injection into the analytical instrument and/or by condensation of the water vapour (only when the partial pressure of the water vapour reaches the equilibrium vapour pressure of water or

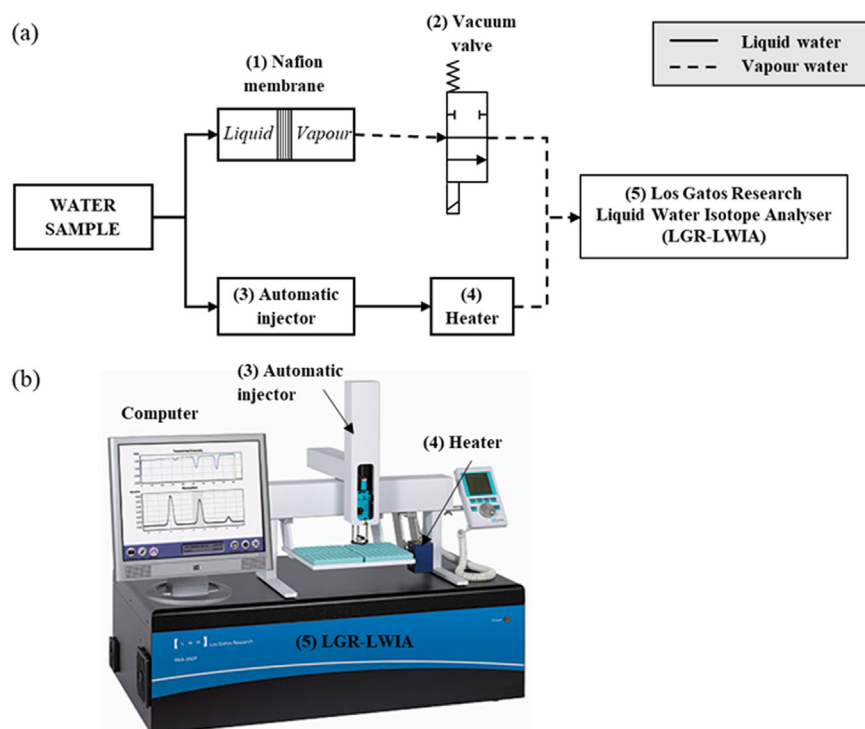


Fig. 1. (a) Schematic diagram of the experimental setup, including (1) the membrane holder unit, (2) the electronic vacuum valve, (3) the automatic injector unit with (4) the attached heater and (5) the Liquid Water Isotope Analyser from Los Gatos Research (LGR-LWIA). Note that the solid lines in the diagram represent liquid water and the dashed lines vapour water. (b) Picture of the LGR-LWIA [61].

above). At steady state, the pressure in the downstream volume of the membrane is kept constant and the water vapour flow-rate injected into the analytical instrument is also constant. Hence, a flowmeter or a syringe for the sample injection is no longer needed. This makes it simple to use Nafion membranes to inject water into analytical instruments such as mass spectrometers or laser-based spectrometers without the need of complex sample preparation for on-line analysis. In addition, there is no need for using thermal heaters to vaporize the liquid water before injections, which reduces the power consumption.

Here we present our recent work that has explored the use of Nafion membranes as a MI inlet system, which can be implemented in field-deployable laser and mass spectrometers used for stable isotope analyses. Von Freyberg et al. [21] have already developed a Continuous Water Sampler Module (CoWS), which uses a Nafion membrane as MI inlet system coupled to a L2130-i Cavity Ring-Down Spectrometer to measure on-line $^2\text{H}/^1\text{H}$ and $^{18}\text{O}/^{16}\text{O}$ isotopic ratios in liquid water directly in the field and at high frequency (30 min). López-Díaz et al. [56] have also measured stable isotopes in water at high frequency using MIMS techniques with a Nafion membrane incorporated into a portable mass spectrometer. Rozenkevich et al. have studied the permeability of a Nafion membrane type for water with various isotopic compositions (H_2^{16}O , HD^{16}O , HT^{16}O , H_2^{18}O) in a system where liquid water was found on both sides of the membrane, and they did not find differences in the permeability [57]. However, it is still poorly understood and poorly characterized how Nafion membranes behave as MI inlet systems, where liquid water is present in the upstream part and water vapour in the downstream part; whether they are influenced by the water quality characteristics; and how this may influence the accuracy of the measurements. Note that even if it is well known that the evaporation of water implies a noticeable isotopic effect and influences the result of the measured isotopic ratios in water [1], we could expect minimal fractionation when using the membrane system, where the water is completely converted into water vapour once it reaches the downstream part of the membrane. This conversion happens because the pressure there is more than one order of magnitude lower than the equilibrium vapour pressure of water. Then the water vapour is directed to the cavity for analysis. Hence, equilibrium fractionation does not take place since there is no liquid-vapour interaction. Kinetic

fractionation could favour the evaporation and diffusion through the membrane of the water with lighter isotopes, as at the same kinetic energy ($E = (mv^2)/2$) the velocity is higher for lighter masses. However, during pervaporation the downstream part of the membrane does not reach the equilibrium vapour pressure of water. Consequently, the water that is converted into the vapour phase will not condense. Eventually, the evaporation process is not affected by the kinetic fractionation. Moreover, the pervaporation process is driven by the difference in pressure at both sides of the membrane and is not limited by diffusion. Therefore, the kinetic fractionation is not likely to happen during the transportation. However, taking into account that Nafion membranes are cation exchange membranes, not only the kinetic fractionation could advantage the transport of the lighter isotopes, but also the equilibrium fractionation could favour the transport of one of the isotopes (i.e. ^{18}O or ^{16}O for $^{18}\text{O}/^{16}\text{O}$ measurements and ^2H or ^1H for $^2\text{H}/^1\text{H}$ measurements). This is because during the equilibrium reactions that could take place in the membrane active layer itself and/or in presence of certain contaminants, the lighter isotope could react faster than the heavy one and/or the heavier isotope could preferentially accumulate in the species or compounds with the higher oxidation state [1]. Hence, these effects would eventually result in altered isotopic ratios.

Here we study the fractionation of the isotopic ratios of $^2\text{H}/^1\text{H}$ and $^{18}\text{O}/^{16}\text{O}$ in liquid water when using a Nafion membrane as a MI inlet system coupled with a laser spectrometer. We compare our results with standard laboratory measurements obtained using an automatic injector and a heater to convert liquid water into vapour water. We examine specifically the effect of pollutant concentration, salinity and membrane thickness on the accuracy and precision of a wide range of water stable isotopic ratio measurements when using a Nafion membrane as a MI inlet system.

2. Experimental work

2.1. Instrumental set up and methods

Fig. 1a shows the schematic diagram of the experimental setup, which consists of (1) a membrane holder unit attached to (2) an

electronic vacuum valve, and (3) an automatic injector unit attached to (4) a heater as inlet systems of (5) a Liquid Water Isotope Analyser from Los Gatos Research (LGR-LWIA; model TIWA-45-EP; Fig. 1b). The LGR-LWIA is operated by the Catchment and eco-hydrology group at the Luxembourg Institute of Science and Technology (LIST). The manufacturer claims a precision of 0.4 and 0.1‰ for $^2\text{H}/^1\text{H}$ and $^{18}\text{O}/^{16}\text{O}$ isotopic ratios, respectively [58].

The automatic injector is a standard unit to introduce liquid water samples into the LGR-LWIA instrument for the isotopic ratio measurements. A Hamilton microliter syringe injects the liquid sample through a PTFE-coated septum (1 μl) in the injection port of the autosampler, where the liquid water is heated ($\sim 85^\circ\text{C}$) and vaporized under vacuum (2 mbar). Then the water vapour is driven into the LGR-LWIA optical cavity through a 1.6 mm internal diameter PTFE tube by the gradient of pressure when the entry valve opens (the LGR-LWIA cavity is at 0.68 mbar). Once the sample enters the optical cavity, the valve is closed and the vacuum in the cavity is constantly kept at 1 mbar. The cavity is thermalized at 40°C . After 34 s of sample equilibration, the device measures the absorption in the near-infrared region of the vapour sample inside the optical cavity from a tuneable diode laser coupled off-axis to a high-finesse optical cavity.

The membrane holder unit consists of two reservoirs separated by a Nafion membrane that has a transport area of 29 mm^2 . We used three Nafion membranes with 1100 equivalent weight and different thicknesses: N-212 (50.8 μm), N-115 (127 μm) and N-1110 (254 μm) from Ion Power GmbH. The upper reservoir is in contact with liquid water while the lower reservoir is connected to the inlet of the LGR-LWIA instrument, whose cavity pressure is kept at 0.68 mbar, through the electronic vacuum valve. The upstream reservoir of the membrane holder is filled completely with the liquid water (sample) to avoid isotopic exchange with air. Water passes through the membrane into the lower reservoir in the form of water vapour due to the pressure difference between the upstream part (upper reservoir, typically at atmospheric pressure and ambient temperature, i.e. 20°C) and the downstream part (lower reservoir, typically as low as 1.2 mbar) created by the vacuum pump system of the LGR-LWIA instrument. The interfacial evaporation takes place due to the low pressure in the downstream part of the membrane, which is much lower than the equilibrium vapour pressure of water at 20°C (~ 23 mbar). As a result, the evaporation rate of the water is always high (for both thin and thick membranes). Moreover, it does not limit the water flux, since there is no liquid water on the surface of the membrane in the downstream part. The water vapour accumulates in the lower reservoir during the equilibration and analysis of the previous sample (34 + 30 s). After the analysis, the LGR-LWIA cavity is flushed with dry air and pumped out. At the same time, the electronic valve is opened twice to pump out the water vapour accumulated in the lower reservoir (the process takes 23 s). Finally, when the pressure in the LGR-LWIA's cavity reaches back to 0.68 mbar, the electronic valve attached to the membrane holder opens during 3.5 s, when the entry valve of the LGR-LWIA instrument is also open. An amount of vapour equivalent to 1 μl of liquid water flows into the cavity of the instrument, driven by the difference in pressure between the membrane holder and the LGR-LWIA's cavity. The LGR-LWIA instrument stabilizes the pressure in the cavity (1 mbar) when the entry valve closes. After 34 s of equilibration, it measures the absorption in the near-infrared region of the water vapour.

Each water sample is analysed twice. The first analysis uses the automatic injector, representing the isotopic ratio of the water without the influence of the membrane (referred to as “Automatic injector” analyses), and the second analysis uses the Nafion membrane as the inlet system (referred to as “Nafion membrane” analyses). We perform the two analyses in sequence for each sample and compare the results to each other in order to study the fractionation of the stable isotopes through Nafion membranes under different conditions. We define the precision of the measurements as the mean of the standard deviations (σ) of the mean values of each measurement, and the average accuracy

as the mean of the absolute difference between the measured isotopic ratio and the isotopic ratio of the different standards (referred to as ‘Real isotopic ratios’). Note that when samples are not standards, that is the case of the three in-house laboratory standards (Mer: desalinated sea water; Belv: distilled tap water from Belvaux in Luxembourg; Cong: water from the freezer), the real isotopic ratios correspond to the values obtained from the calibration of these in-house standards with the LGR-LWIA related to SLAP2 (Standard Light Antarctic Precipitation 2) [59].

The isotopic ratio measurement procedures for the LGR-LWIA analysis are identical for the ‘Nafion membrane’ analyses and the ‘Automatic injector’ analyses. Each sample is analysed ten times and the first five measurements are discarded to eliminate memory effects and to be sure that a steady state has been reached. Before introducing a new sample, the cavity is flushed with dry air and pumped out to remove the remaining old sample in the system. Moreover, for ‘Nafion membrane’ analyses, the old sample is removed from the membrane by flushing the upper reservoir with Argon gas. The upper reservoir is filled with a new sample and a complete isotopic ratio measurement is carried out. The first of the 10 analyses is done with a first sample, which is then removed from the upper reservoir by an Argon gas flush to be sure that no memory effect remains. Then the upper reservoir of the membrane is filled with the same sample a second time to perform the remaining nine analyses. Between analyses, at the same time that the cavity of the LGR-LWIA instrument is flushed with the dry air and pumped out to remove the remaining old sample, the electronic vacuum valve is opened twice, during 3.5 s each time, to pump out the vapour accumulated in the lower part reservoir of the membrane holder. The complete process (including the analysis of the vapour sample) takes 1.5 min. From these nine analyses, the first four are discarded to exclude any memory effect and to allow for steady state to be reached. This may eventually warrant that the measured isotopic ratio corresponds to the analysed sample.

Taking into account that the membranes were preconditioned at 23°C and 50% RH, the initial membrane water content was equal to 5% of their dry basis weight. According to the technical data sheet from the manufacturer [60], the water uptake from a dry membrane to a conditioned membrane at 100°C for 1 h is the 50% of its dry basis weight (100 g/m^2) for N-212, and 38% of their dry basis weight for N-115 and N-1110 (250 and 500 g/m^2 , respectively). It means that the initial water contents of the N-212, N-115 and N-1110 membranes are 0.145 μl , 0.3625 μl and 0.725 μl , respectively, while the water uptakes at 100°C during one hour are 1.45 μl , 2.755 μl and 5.51 μl , respectively. In our pervaporation system, taking into account the volume of water that is evacuated in the cleaning process between samples and that the first five samples are discarded, we can assume that we have reached the steady state at 20°C before the last five measurements are carried out, since an amount of water of more than ten times the water uptake of the membranes might have passed through the membranes.

2.2. Sample preparation

We used different water samples with different matrices. Specifically, we used four groups of samples: (1) samples without matrix (i.e. standards), (2) natural samples (including in-house laboratory standards and samples collected in the field), (3) mixtures of natural sample matrices (i.e. obtained by evaporation) and standard samples, and (4) solutions of sea salts.

The group of samples without matrix includes seven water standard samples from Los Gatos Research (LGR): 1, 1C, 2C, 3C, 3, 4C, 5C. We used these water standards to study the possibility that the different stable isotopes could be fractionated through the Nafion membranes depending on the abundance of the heavy isotope.

The group of natural samples includes three in-house laboratory standards (Mer: desalinated sea water; Belv: distilled tap water from Belvaux in Luxembourg; Cong: water from the freezer) and five samples collected in the field (Rain: rainfall water collected in Oberpallen

(western Luxembourg); Wei, WeiF: two streamwater samples from the Weierbach stream; Use, UseF: two streamwater samples from the Attert River at Useldange (western Luxembourg)). Both streamwater samples were collected manually and filtered with a 0.45 μm filter (Wei, Use) and with a 0.02 μm filter (WeiF, UseF), following the standard sample preparation procedure for the LGR-LWIA instrument [62]. The latter has the pore size closer to the size of the Nafion membrane water channels ($\sim 0.0025 \mu\text{m}$) and was used to verify if potential fractionation is due to a physical phenomenon (e.g. filtering channel size) or if it is rather due to a combination of both physical and chemical phenomena (e.g. interaction of anions from the membrane internal structure with molecules having positive charge or positive density of charge). Note that the Weierbach headwater catchment (0.45 km^2) is mainly covered by deciduous forest [63]. It drains south into the Attert River, a left tributary of the Alzette River in Luxembourg. Its water has low salinity and high organic matter content. The Attert River sample was collected at the Useldange streamgauge (245 km^2). The basin is almost equally covered by forest, grassland and cultivated land [64]. The Attert streamwater is characterized by high salinity and high levels of pollution, mainly nitrates and phosphates from the surrounding cultivated lands. These samples were measured to study the influence of the matrix on the isotopic ratio fractionation through the Nafion membranes.

The analysis of the group of mixtures of natural sample matrices and standards aimed at verifying whether matrices would produce deviations in the isotopic ratios of the standard samples. The group of samples include the matrices of the natural samples: Rain, Wei and Use. Each sample was first evaporated in five 2-ml vials to concentrate their matrix. Then the matrix left in each vial was solved with one of the five different standards (1, 2C, 3C, 4C, 5/5C) to create fifteen new samples containing three different matrix types with five different isotopic ratios: 1R, 2CR, 3CR, 4CR, 5CR, 1W, 2CW, 3CW, 4CW, 5W, 4CWF, 1U, 2CU, 3CU, 4CU, 5CU, 4CUF. Note that for one sample the LGR standard 5 was used instead of the 5C for availability reasons. Also, for these samples we considered the real isotopic values as the values reported for the standards (i.e. without the matrix).

The group of solutions of sea salts aimed at studying whether the cation exchange with the salts could favour the transport of one of the two isotopes through the different membranes. Seventeen solutions were prepared with distilled water and standard sea salts from Sigma Aldrich. The salinity in the solutions ranged from 0 to 38 mg/ml. Concentrations range from river water salinity ($< 0.5 \text{ mg/ml}$) to sea water salinity ($\sim 38 \text{ mg/ml}$).

3. Results and discussion

3.1. Water samples with a wide range of heavy isotopes abundances

The real isotopic ratios of the water standards cover a wide range of values, from $-154 \pm 0.5\text{‰}$ to $-9.2 \pm 0.5\text{‰}$ for $^2\text{H}/^1\text{H}$ and from $-19.57 \pm 0.1\text{‰}$ to $-2.69 \pm 0.15\text{‰}$ for $^{18}\text{O}/^{16}\text{O}$ isotopic ratios. Fig. 2 shows the isotopic ratios of $^2\text{H}/^1\text{H}$ (Fig. 2a) and $^{18}\text{O}/^{16}\text{O}$ (Fig. 2b) of the seven standards for both the “automatic injector” and the “Nafion membrane” analysis, as described in Section 2. The real isotopic ratios of the standards are also plotted in Fig. 2 in order to validate the accuracy of the measurements in both cases. The results show that there is no significant change in the isotopic ratios for the “Nafion membrane” analysis compared to both their real isotopic ratio values and the “automatic injector” results.

The use of Nafion membranes did not influence the precision of the measurements (shown in Table 1 and 2). However, the precision was slightly worse when using the thickest membrane (N-1110) for the $^2\text{H}/^1\text{H}$ isotopic ratio. All measured values were in the same range for both measurements with “automatic injector” and “Nafion membranes”. The precision ranged between 0.177‰ and 0.349‰ and between 0.042‰ and 0.077‰ for $^2\text{H}/^1\text{H}$ and $^{18}\text{O}/^{16}\text{O}$ isotopic ratios, respectively. The mean of the absolute difference between the isotopic

ratios of the water standard samples of the “automatic injector” and “Nafion membranes” analysis (shown in Table 1 and 2) ranged between 1.103‰ and 2.406‰ for $^2\text{H}/^1\text{H}$ isotopic ratios, and between 0.150‰ and 0.499‰ for $^{18}\text{O}/^{16}\text{O}$ isotopic ratios. In both cases, the values were slightly worse for the thickest membrane (N-1110). The average accuracy (shown in Table 1 and Table 2) was similar in both the “automatic injector” and the “Nafion membranes” analyses, ranging between 0.702‰ and 1.143‰ and between 0.127‰ and 0.307‰ for the $^2\text{H}/^1\text{H}$ and $^{18}\text{O}/^{16}\text{O}$ isotopic ratios, respectively. No trend on membrane thickness or heavy isotope concentration was observed. However, lower accuracies were associated to the use of the thickest membrane (N-1110: 1.992 and 0.363‰ for the $^2\text{H}/^1\text{H}$ and $^{18}\text{O}/^{16}\text{O}$ isotopic ratios, respectively).

The measured accuracy for all the analyses using the membranes N-212 and N-115 remained within the error range of the LGR-LWIA instrument, indicating that no fractionation occurred through the membranes. However, the use of the thickest membrane (N-1110, 254 μm) resulted in a lower accuracy and precision, suggesting that fractionation might occur. We believe that thicker membranes might affect the homogeneity of the water molecules transport through its thicker hydrophobic layers and hence worsening the accuracy and precision of the measurements. Therefore, we do not recommend the use of thick membranes (e.g. N-1110; i.e. more than $\sim 150 \mu\text{m}$) for O and H isotopic ratio analysis in water.

3.2. Water samples with different matrices

Fig. 3, Table 1 and Table 2 show the measured isotopic ratios of the water samples with different matrices for both the “automatic injector” and “Nafion membranes” analyses. Results clearly show that the matrices did not affect the precision of the isotopic ratio analyses, which was close to the precision obtained for the standards without matrix. The mean precision ranged between 0.249‰ and 0.409‰ and between 0.053‰ and 0.098‰ for $^2\text{H}/^1\text{H}$ and $^{18}\text{O}/^{16}\text{O}$ isotopic ratios, respectively. Nonetheless, results show that the absolute difference between the isotopic ratios of “automatic injector” and “Nafion membranes” samples containing matrix was slightly larger than absolute differences obtained when measuring the standard samples without matrix (see Section 3.1). The mean values ranged between 0.779‰ and 1.802‰ and between 0.357‰ and 0.538‰ for $^2\text{H}/^1\text{H}$ and $^{18}\text{O}/^{16}\text{O}$ isotopic ratios, respectively.

We observed a larger difference between the “automatic injector” and the “Nafion membranes” analyses when using the thickest membrane (N-1110) than when using the other two membranes. In most of the cases, the accuracies for the samples Cong, Belv and Mer were also worse than those of the standards without matrix. Furthermore, we did not observe any difference in the accuracy when changing the type of matrix, or when increasing membrane thickness. Average accuracies ranged between 0.595‰ and 1.812‰ for $^2\text{H}/^1\text{H}$ isotopic ratios, being worse when using the N-1110 membrane (2.303‰). Accuracies ranged between 0.157‰ and 1.073‰ for the $^{18}\text{O}/^{16}\text{O}$ isotopic ratios. We did not find significant differences in the analyses when comparing samples filtered at 0.45 or 0.02 μm .

Fig. 4, Table 1 and Table 2 show the isotopic ratio measurements of the samples matrices mixed with the standards. For the three matrices (i.e. evaporated rain, streamwater from the Weierbach catchment and from the Attert River at Useldange), the precision of the “Nafion membranes” measurements (between 0.168‰ and 0.455‰ and 0.039–0.089‰ for $^2\text{H}/^1\text{H}$ and $^{18}\text{O}/^{16}\text{O}$ isotopic ratios, respectively) was better than for the “automatic injector” measurements (between 0.513‰ and 0.964‰ and 0.168–0.455‰ for $^2\text{H}/^1\text{H}$ and $^{18}\text{O}/^{16}\text{O}$ isotopic ratios, respectively). This behaviour is significantly different compared to the previous experiments using the standards without matrix and the samples with different matrices. This could be related to the evaporation process during the sample preparation. We hypothesize that during the total evaporation of the water in the vials some soluble

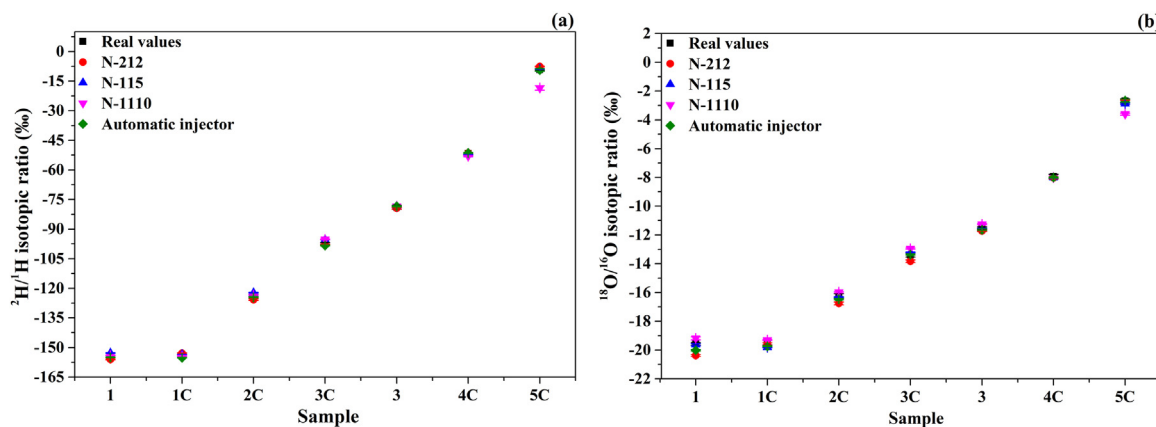


Fig. 2. Real isotopic ratios of different LGR standard samples (1, 1C, 2C, 3C, 3, 4C, 5C), and values measured when using three Nafion membranes of different thickness (N-212, N-115, N-1110) and an automatic injector: a) $^2\text{H}/^1\text{H}$ isotopic ratios and b) $^{18}\text{O}/^{16}\text{O}$ isotopic ratios.

components in the matrices could become insoluble, forming suspensions when dissolving them again with the standards. Consequently, the membranes would act as filters, preventing insoluble matter from entering the LGR-LWIA instrument. Therefore, the use of Nafion membranes could limit the data dispersion (due to the presence of insoluble matter unfiltered in the analysis chamber), in comparison to the direct sample injection using the automatic injection unit with the conventional filters. The precision of the $^{18}\text{O}/^{16}\text{O}$ isotopic ratio measurements in the samples containing the matrices extracted from the rain and the Weierbach streamwater did not depend on the membrane thickness, while measurement precision is slightly improved when increasing the membrane thickness for the samples containing the Atttert River matrix, which is richer in salts and pollutants. $^2\text{H}/^1\text{H}$ isotopic ratios did not show any specific precision trend for the different matrices, but measurements were more precise when using the medium thickness membrane (N-115; all matrices).

The average absolute differences of $^{18}\text{O}/^{16}\text{O}$ isotopic ratios for the “automatic injector” and the “Nafion membranes” analyses ranged between 0.128‰ and 0.548‰ for all matrices. Nevertheless, the behaviour was different depending on the matrix. The samples containing the rainfall matrix showed larger absolute differences when using the thickest membrane (N-1110), whereas the largest absolute differences for the samples containing the Atttert River matrix (high salt and pollution content) were found using the thinnest membrane (N-212), pointing towards more depleted values. We did not find any trend for the samples containing the Weierbach streamwater matrix (high content in organic matter). We observed the same behaviour for the accuracy (in absolute values). Values ranged between 0.075‰ and 0.173‰ for the samples containing the rainfall matrix, except for the thickest membrane (0.598‰); between 0.112‰ and 0.336‰ for the samples containing the Weierbach streamwater matrix and between 0.160‰ and 0.265‰ for the samples containing the Atttert streamwater matrix, except for the thinnest membrane (0.509‰). On the contrary, the $^2\text{H}/^1\text{H}$ isotopic ratios showed a different behaviour. The absolute differences for the “automatic injector” and the “Nafion membranes” analyses, except for the thickest membrane, ranged between 0.483‰ and 1.079‰ for the samples containing the rainfall matrix and between 0.837‰ and 1.809‰ for the samples containing the Atttert streamwater matrix, being in both cases the worst results obtained when using the thickest membrane (1.563 and 2.308‰, respectively). Along similar lines, the accuracies in absolute values exhibited the same patterns, ranging (with except of the thickest membrane) from 0.755‰ to 0.964‰ for the samples containing the rainfall matrix and between 0.513‰ and 1.612‰ for the samples containing the Atttert streamwater matrix. We did not find any major difference between the “automatic injector” and the “Nafion membranes” results, except when using the thickest membrane, for which the accuracies were 2.268 and 1.795‰,

respectively. The samples containing the Weierbach streamwater matrix exhibited an opposite trend, where the absolute difference for the “automatic injector” and the “Nafion membranes” analyses ranged between 0.718‰ and 0.731‰, the difference being larger when using the thinnest membrane (1.223‰). Similar results were observed for the accuracies, ranging (except for the thinnest membrane) between 0.576‰ and 0.910‰. We did not find any major difference between the “automatic injector” and the “Nafion membranes” results using the N-115 and N-1110 membranes. However, the accuracy was lower when using the thinnest membrane N-212 (1.640‰).

The samples containing the matrix from the rainfall showed similar values to those of the standards without matrix for both isotopic ratios. This is most probably due to the poor content of the matrix. We did not observe fractionation when using the N-212 and N-115 membranes (50.8 and 127 μm thickness). However, results were worse when using the thickest membrane (N-1110; 254 μm). The results were different for the other two matrices. The samples containing the Weierbach streamwater matrix, with high content in organic matter and low content in pollutants and salts, did not show any trend in the $^{18}\text{O}/^{16}\text{O}$ isotopic ratios. However, results were less accurate for the $^2\text{H}/^1\text{H}$ isotopic ratios when using the thinnest membrane, and the accuracy when using the thickest membrane was better than the one of the “automatic injector” analysis. This could be explained by the high content of hydrogen in the organic matter, which could potentially be exchanged with deuterium, resulting in worse accuracy and precision. Compared to the thicker membrane, it is the thinner membrane that might be more prone to transfer the organic matter (even larger molecules) through the hydrophobic part until the active layer. This fact facilitates the hydrogen/deuterium exchange (as the active groups of the membrane are anions (RSO_3^-) and the hydrogens cations) resulting in worst accuracies. No trend was observed for $^{18}\text{O}/^{16}\text{O}$ isotopic ratios, most probably because the membrane's active groups do not facilitate oxygen exchange with the organic matter (both, the active groups and the oxygen, are anions), so less interference is likely to occur.

We observed a different behaviour for the samples containing the Atttert streamwater matrix, which has a high content of salts and pollutants. In this case, the charged ions from the salts and pollutants, together with a high content of nitrates [64], could potentially pass through the membrane, as they are solvated by water. Nevertheless, it could be more difficult for some large negative ions, like NO_3^- and SO_4^{2-} , to be transported through the membrane, hindering the transportation of the heavier isotopes and resulting in fractionation. Thicker membranes are not only harder to pass, but also expected to be more selective to water molecules, enhancing the retention of large negative ions, most probably in the upper part of the membrane structure. This could explain why we obtained better accuracies and precisions when using thicker membranes for $^{18}\text{O}/^{16}\text{O}$ isotopic ratios in samples with

Table 1

Average values and standard deviations of five $\delta^{18}\text{O}$ measurements of Los Gatos Research (LGR) water standards (1, 1C, 2C, 3C, 3, 4C, 5C), manually collected natural waters (Mer, Belv, Cong, Rain, Wei, WeiF, Use, UseF), artificial samples created dissolving matrices from the manually collected samples in LGR water standards (xR, Xw, xU, being x each used standard), and seventeen solutions with sea salt concentration ranging from 0 to 38 mg/ml. AVG: average of the standard deviations; AVG-accuracy: average of the accuracies; AVG(1–6): average of the standard deviations (AVG) of the first six samples, corresponding to the range of salt concentration in rivers; Diff. N-212, Diff. N-115 and Diff. N-1110: difference between the “automatic injector” and the “Nafion membranes” values; SD: standard deviations associated to values shown on the previous column.

Sample	Real $\delta^{18}\text{O}$	SD	$\delta^{18}\text{O}$ Automatic injector	SD	$\delta^{18}\text{O}$ N-212	SD	$\delta^{18}\text{O}$ N-115	SD	$\delta^{18}\text{O}$ N-1110	SD	Diff. N-212	Diff. N-115	Diff. N-1110
Los Gatos Research (LGR) water standards													
1	−19.57	0.1	−20.016	0.053	−20.376	0.057	−19.628	0.078	−19.186	0.108	−0.36	0.388	0.83
1C	−19.49	0.15	−19.737	0.041	−19.577	0.083	−19.805	0.035	−19.298	0.037	0.159	−0.069	0.439
2C	−16.24	0.15	−16.471	0.036	−16.759	0.096	−16.322	0.025	−15.977	0.049	−0.288	0.15	0.495
3C	−13.39	0.15	−13.361	0.045	−13.823	0.095	−13.217	0.03	−12.951	0.043	−0.462	0.144	0.409
3	−11.54	0.1	−11.635	0.051	−11.716	0.042	−11.549	0.027	−11.262	0.041	−0.081	0.085	0.373
4C	−7.94	0.15	−7.999	0.042	−8.035	0.086	−8.005	0.049	−8.013	0.024	−0.036	−0.006	−0.013
5C	−2.69	0.15	−2.673	0.104	−2.725	0.083	−2.879	0.052	−3.605	0.07	−0.052	−0.207	−0.932
AVG				0.053		0.077		0.042		0.053	0.205	0.15	0.499
AVG-accuracy			0.161		0.307		0.127		0.363				
Manually collected water samples													
Cong	−17.03	0.25	−17.993	0.06	−18.042	0.185	−16.63	0.064	−16.327	0.1	−0.048	1.364	1.666
Belv	−7.9	0.16	−7.825	0.068	−9.303	0.076	−7.95	0.046	−8.083	0.054	−1.478	−0.125	−0.258
Mer	0.42	0.36	0.312	0.162	1.224	0.099	0.441	0.076	0.061	0.068	0.912	0.129	−0.251
Wei	−	−	−7.508	0.063	−6.695	0.11	−7.208	0.048	−7.675	0.054	0.812	0.3	−0.168
WeiF	−	−	−7.808	0.046	−7.924	0.028	−7.528	0.029	−7.123	0.041	−0.117	0.279	0.685
Use	−	−	−7.537	0.093	−7.44	0.106	−7.446	0.069	−7.81	0.029	0.098	0.091	−0.273
UseF	−	−	−7.68	0.047	−7.832	0.099	−7.529	0.046	−7.659	0.039	−0.151	0.152	0.021
Rain	−	−	−14.704	0.046	−15.056	0.083	−14.289	0.073	−13.724	0.036	−0.352	0.415	0.98
AVG				0.073		0.098		0.056		0.053	0.496	0.357	0.538
AVG-accuracy			0.382		1.073		0.157		0.415				
Artificial samples created dissolving matrices from the manually collected samples in LGR water standards													
1R	−19.57	0.1	−19.915	0.164	−19.569	0.043	−19.667	0.049	−20.116	0.102	0.346	0.248	−0.201
2CR	−16.24	0.15	−16.335	0.176	−16.173	0.05	−16.484	0.05	−16.87	0.036	0.162	−0.149	−0.537
3CR	−13.39	0.15	−13.411	0.161	−13.261	0.057	−13.442	0.081	−14.04	0.063	0.151	−0.031	−0.629
4CR	−7.94	0.15	−7.716	0.143	−7.774	0.061	−7.897	0.057	−7.482	0.052	−0.058	−0.18	0.234
5CR	−2.69	0.15	−2.512	0.214	−2.678	0.077	−2.972	0.037	−1.984	0.056	−0.166	−0.46	0.528
AVG				0.172		0.058		0.055		0.062	0.177	0.214	0.426
AVG-accuracy			0.173		0.075		0.144		0.598				
1W	−19.57	0.1	−19.616	0.22	−19.71	0.065	−20.357	0.038	−19.592	0.132	−0.094	−0.741	0.024
2CW	−16.24	0.15	−16.582	0.183	−16.4	0.049	−16.846	0.058	−16.326	0.07	0.182	−0.263	0.257
3CW	−13.39	0.15	−13.337	0.199	−13.492	0.083	−13.7	0.052	−13.49	0.055	−0.155	−0.362	−0.152
4CW	−7.94	0.15	−7.747	0.123	−8.009	0.113	−7.833	0.072	−7.908	0.069	−0.261	−0.085	−0.161
5CW	−2.69	0.15	−2.854	0.093	−2.855	0.08	−2.658	0.081	−2.541	0.074	−0.001	0.196	0.313
4CWF	−7.94	0.15	−7.537	0.082	−7.46	0.067	−7.766	0.049	−7.656	0.037	0.077	−0.23	−0.12
AVG				0.15		0.076		0.058		0.073	0.128	0.313	0.171
AVG-accuracy			0.2		0.186		0.336		0.112				
1U	−19.57	0.1	−19.982	0.183	−19.231	0.138	−20.197	0.063	−19.625	0.062	0.752	−0.215	0.358
2CU	−16.24	0.15	−16.442	0.323	−16.93	0.123	−16.797	0.069	−16.475	0.044	−0.488	−0.356	−0.033
3CU	−13.39	0.15	−13.63	0.281	−13.976	0.038	−13.709	0.045	−13.62	0.025	−0.346	−0.079	0.011
4CU	−7.94	0.15	−7.866	0.219	−8.483	0.059	−7.903	0.046	−8.046	0.056	−0.617	−0.037	−0.18
5CU	−2.69	0.15	−2.593	0.259	−3.177	0.071	−2.659	0.02	−2.831	0.019	−0.583	−0.065	−0.237
4CUF	−7.94	0.15	−7.841	0.087	−8.347	0.106	−7.961	0.057	−7.746	0.03	−0.505	−0.12	0.095
AVG				0.225		0.089		0.05		0.039	0.548	0.145	0.152
AVG-accuracy			0.187		0.509		0.265		0.16				
Salinity solutions													
Concentration (mg/ml)													
0			−8.014	0.039	−7.806	0.076	−8.584	0.042	−7.287	0.041	0.208	−0.57	0.727
0.05			−7.977	0.035	−7.666	0.071	−7.962	0.064	−7.824	0.052	0.311	0.015	0.153
0.07			−7.801	0.091	−7.536	0.054	−8.143	0.052	−7.92	0.072	0.265	−0.342	−0.119
0.2			−7.437	0.154	−7.929	0.089	−8.224	0.07	−7.832	0.026	−0.492	−0.787	−0.395
0.47			−7.296	0.131	−7.767	0.095	−7.965	0.092	−8.016	0.048	−0.471	−0.669	−0.72
0.76			−7.479	0.141	−7.767	0.055	−8.05	0.04	−7.512	0.053	−0.288	−0.571	−0.034
1.9			−7.623	0.089	−7.862	0.102	−7.565	0.078	−8.283	0.081	−0.239	0.058	−0.66
3.98			−7.869	0.137	−8.185	0.081	−7.574	0.071	−8.368	0.025	−0.316	0.295	−0.499
7.66			−8.344	0.071	−8.182	0.071	−7.805	0.072	−7.708	0.054	0.162	0.539	0.635
11.3			−8.34	0.039	−8.292	0.044	−9.646	0.046	−8.002	0.07	0.048	−1.306	0.338
15.03			−7.924	0.133	−7.983	0.068	−9.091	0.081	−8.384	0.076	−0.059	−1.167	−0.461
19.2			−7.764	0.089	−7.92	0.063	−8.898	0.05	−7.974	0.023	−0.156	−1.133	−0.21
22.76			−7.689	0.058	−8.259	0.072	−8.623	0.088	−7.945	0.049	−0.571	−0.934	−0.256
26.63			−8.422	0.047	−7.971	0.04	−8.397	0.109	−7.576	0.05	0.451	0.026	0.846
30.36			−8.35	0.069	−8.123	0.049	−8.135	0.083	−7.605	0.063	0.227	0.215	0.745
34.23			−8.091	0.12	−8.076	0.059	−8.362	0.021	−7.877	0.053	0.015	−0.271	0.214
37.9			−7.762	0.097	−8.057	0.044	−8.242	0.063	−8.511	0.117	−0.294	−0.48	−0.749
AVG				0.091		0.067		0.066		0.056	0.269	0.552	0.457
AVG(1–6)				0.098		0.073		0.06		0.049	0.339	0.492	0.358

Table 2

Average values and standard deviations of five $\delta^2\text{H}$ measurements of Los Gatos Research (LGR) water standards (1, 1C, 2C, 3C, 3, 4C, 5C), manually collected natural waters (Mer, Belv, Cong, Rain, Wei, WeiF, Use, UseF), artificial samples created dissolving matrices from the manually collected samples in LGR water standards (xR, Xw, xU, being x each used standard), and seventeen solutions with sea salt concentration ranging from 0 to 38 mg/ml. AVG: average of the standard deviations; AVG-accuracy: average of the accuracies; AVG(1–6): average of the standard deviations (AVG) for the first 6 samples, corresponding to the range of salt concentration in rivers; Diff. N-212, Diff. N-115 and Diff. N-1110: difference between the “automatic injector” and the “Nafion membranes” values; SD: standard deviations associated to values shown on the previous column.

Sample	Real $\delta^2\text{H}$	SD	$\delta^2\text{H}$ automatic injector	SD	$\delta^2\text{H}$ N-212	SD	$\delta^2\text{H}$ N-115	SD	$\delta^2\text{H}$ N-1110	SD	Diff N-212	Diff N-115	Diff N-1110
Los Gatos Research (LGR) water standards													
1	−154.10	0.10	−154.960	0.128	−156.033	0.249	−152.770	0.189	−154.000	0.152	−1.073	2.190	0.960
1C	−154.00	0.50	−155.171	0.143	−152.929	0.269	−153.567	0.156	−154.272	0.257	2.242	1.604	0.898
2C	−123.70	0.50	−124.598	0.284	−125.760	0.389	−122.282	0.183	−123.491	0.421	−1.162	2.316	1.107
3C	−97.30	0.50	−98.361	0.226	−97.952	0.318	−95.397	0.096	−95.246	0.167	0.409	2.964	3.115
3	−79.00	1.00	−78.457	0.277	−79.465	0.376	−78.516	0.232	−78.391	0.088	−1.008	−0.059	0.066
4C	−51.60	0.50	−51.411	0.226	−51.377	0.240	−52.158	0.257	−53.003	0.242	0.033	−0.747	−1.592
5C	−9.20	0.50	−9.393	0.619	−7.600	0.201	−8.876	0.127	−18.497	1.118	1.792	0.516	−9.105
AVG				0.271		0.292		0.177		0.349	1.103	1.485	2.406
AVG-accuracy			0.702		1.143		0.921		1.992				
Manually collected water samples													
Cong	−96.88	0.28	−96.022	0.100	−93.678	0.362	−95.264	0.142	−93.978	0.530	2.344	0.757	2.044
Belv	−51.95	0.34	−52.755	0.226	−52.448	0.238	−52.469	0.230	−53.425	0.352	0.307	0.287	−0.669
Mer	1.62	0.47	1.743	0.318	−0.117	0.734	1.777	0.545	−0.914	1.021	−1.860	0.034	−2.658
Wei	−	−	−50.304	0.427	−46.383	0.315	−46.534	0.120	−51.360	0.449	3.921	3.769	−1.056
WeiF	−	−	−49.810	0.251	−51.576	0.315	−48.678	0.286	−47.510	0.102	−1.767	1.132	2.300
Use	−	−	−50.689	0.140	−50.171	0.254	−50.878	0.289	−51.806	0.276	0.518	−0.190	−1.117
UseF	−	−	−50.366	0.329	−51.186	0.289	−50.392	0.237	−50.537	0.293	−0.820	−0.026	−0.171
Rain	−	−	−107.150	0.426	−108.898	0.163	−107.186	0.146	−102.751	0.252	−1.748	−0.036	4.399
AVG				0.277		0.334		0.249		0.409	1.661	0.779	1.802
AVG-accuracy			0.595		1.812		0.764		2.304				
Artificial samples created dissolving matrices from the manually collected samples in LGR water standards													
1R	−154.10	1.00	−156.106	0.882	−155.305	0.196	−155.541	0.180	−155.783	0.696	0.801	0.565	0.323
2CR	−123.70	0.50	−125.253	0.768	−124.057	0.488	−124.433	0.132	−126.866	0.193	1.196	0.821	−1.613
3CR	−97.30	0.50	−98.237	0.810	−97.132	0.449	−97.891	0.156	−101.140	0.279	1.105	0.346	−2.903
4CR	−51.60	0.50	−51.891	0.914	−50.947	0.356	−52.272	0.127	−51.155	0.518	0.945	−0.381	0.736
5R	−9.20	0.50	−9.235	1.596	−7.889	0.524	−9.536	0.247	−6.994	0.591	1.346	−0.301	2.241
AVG				0.994		0.403		0.168		0.455	1.079	0.483	1.563
AVG-accuracy			0.964		0.739		0.755		2.268				
1W	−154.10	1.00	−155.618	1.492	−155.335	0.132	−155.707	0.094	−154.449	0.697	0.283	−0.088	1.169
2CW	−123.70	0.50	−123.206	1.210	−125.689	0.316	−124.795	0.201	−124.198	0.247	−2.483	−1.588	−0.992
3CW	−97.30	0.50	−98.525	1.298	−99.088	0.468	−98.067	0.137	−98.404	0.227	−0.563	0.458	0.120
4CW	−51.60	0.50	−53.245	0.721	−53.123	0.315	−52.496	0.174	−51.870	0.553	0.122	0.749	1.375
5CW	−9.20	0.50	−9.043	1.116	−9.719	0.496	−9.078	0.215	−8.824	0.411	−0.676	−0.035	0.219
4CWF	−51.60	0.50	−52.024	1.011	−48.812	0.219	−50.554	0.188	−52.460	0.437	3.212	1.470	−0.436
AVG				1.141		0.324		0.168		0.429	1.223	0.731	0.718
AVG-accuracy			0.910		1.640		0.922		0.576				
1U	−154.10	1.00	−153.316	1.710	−151.661	0.660	−155.313	0.103	−155.317	0.362	1.655	−1.996	−2.001
2CU	−123.70	0.50	−123.559	1.519	−125.001	0.395	−124.804	0.305	−126.451	0.501	−1.442	−1.245	−2.891
3CU	−97.30	0.50	−96.580	1.726	−98.016	0.212	−97.698	0.145	−100.011	0.482	−1.436	−1.118	−3.432
4CU	−51.60	0.50	−51.014	1.304	−52.209	0.288	−50.859	0.205	−53.843	0.461	−1.195	0.155	−2.829
5CU	−9.20	0.50	−9.040	1.471	−8.444	0.258	−8.581	0.222	−10.920	0.538	0.596	0.459	−1.880
4CUF	−51.60	0.50	−50.914	0.750	−55.443	0.594	−50.864	0.047	−51.728	0.148	−4.529	0.050	−0.814
AVG				1.413		0.401		0.171		0.415	1.809	0.837	2.308
AVG-accuracy			0.513		1.612		0.802		1.795				
Salinity solutions													
Concentration (mg/ml)													
0.00			−51.593	0.202	−53.834	0.268	−57.696	0.377	−48.277	0.336	−2.241	−6.103	3.316
0.05			−51.267	0.211	−52.028	0.297	−52.466	0.217	−55.946	0.512	−0.760	−1.199	−4.679
0.07			−51.304	0.218	−51.610	0.157	−51.764	0.086	−53.410	0.332	−0.306	−0.460	−2.106
0.20			−51.206	0.256	−54.030	0.210	−54.476	0.227	−51.341	0.187	−2.825	−3.270	−0.136
0.47			−51.118	0.281	−52.095	0.208	−52.351	0.180	−51.736	0.125	−0.977	−1.234	−0.618
0.76			−51.135	0.163	−51.501	0.048	−51.916	0.141	−47.967	0.238	−0.366	−0.781	3.168
1.90			−51.189	0.232	−50.435	0.215	−48.515	0.248	−51.370	0.293	0.755	2.674	−0.181
3.98			−51.164	0.299	−51.384	0.406	−50.963	0.226	−51.126	0.110	−0.220	0.201	0.038
7.66			−51.360	0.214	−51.218	0.319	−51.679	0.144	−52.771	0.283	0.142	−0.320	−1.411
11.30			−52.418	0.259	−56.003	0.210	−60.329	0.204	−51.990	0.328	−3.585	−7.911	0.428
15.03			−52.370	0.362	−52.701	0.122	−56.381	0.236	−54.188	0.159	−0.330	−4.010	−1.817
19.20			−52.719	0.409	−51.904	0.143	−54.908	0.246	−51.437	0.162	0.815	−2.189	1.282
22.76			−52.265	0.326	−53.760	0.390	−55.821	0.310	−51.305	0.322	−1.496	−3.556	0.960
26.63			−51.320	0.237	−51.819	0.201	−53.782	0.302	−47.904	0.380	−0.498	−2.462	3.417
30.36			−51.239	0.351	−52.374	0.259	−52.544	0.234	−49.745	0.249	−1.135	−1.305	1.494
34.23			−50.869	0.384	−50.956	0.094	−55.221	0.454	−50.341	0.189	−0.087	−4.353	0.528
37.90			−51.725	0.315	−51.233	0.271	−53.206	0.248	−58.898	0.637	0.492	−1.481	−7.172
AVG				0.278		0.225		0.240		0.285	1.002	2.559	1.926
AVG(1–6)				0.222		0.198		0.205		0.288	1.246	2.174	2.337

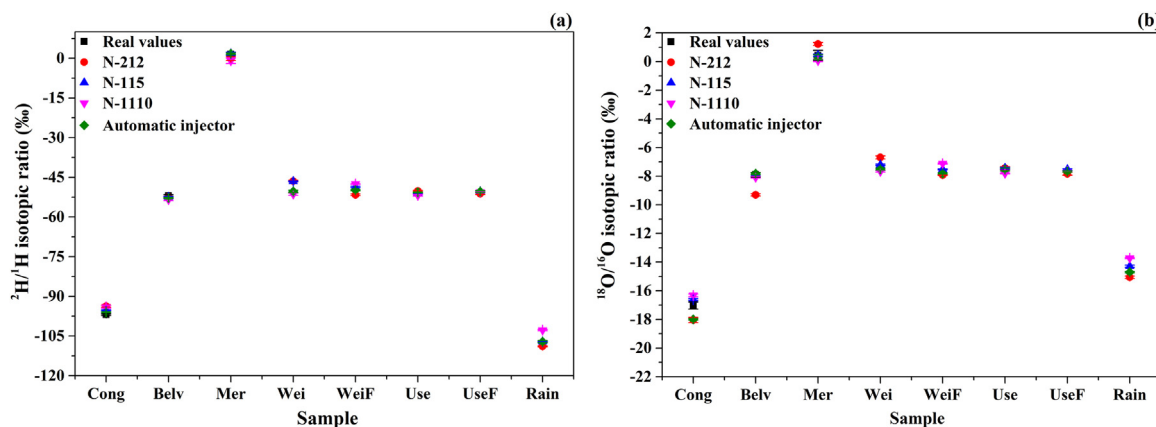


Fig. 3. Isotopic ratios of samples with different matrices measured using three Nafion membranes of different thickness (N-212, N-115, N-1110) and an automatic injector: a) $^2\text{H}/^1\text{H}$ isotopic ratios and b) $^{18}\text{O}/^{16}\text{O}$ isotopic ratios.

high content of salts and pollutants. Nonetheless, when using the thickest membrane and the automatic injector, we observed that the accuracies were similar. This supports the hypothesis that thinner membranes fractionate water isotopic ratios in the presence of large negative ions, either because they create a network of ions that hinders the passage through the membrane to the larger atoms as the oxygen, or because there is oxygen exchange with the solvated ions in the structure of the membrane. On the contrary, hydrogen isotopes might be easily transported, as they are smaller and less prone to be affected by the ions that are present in the structure. Even if there is cation exchange with cations from the salts or pollutants, it does not affect the $^2\text{H}/^1\text{H}$ isotopic ratio. The reason could be a non-preference in the cation exchange for one of the isotopes, being even an advantage that favours together with the active layer of the membrane the passage of both hydrogen isotopes.

3.3. Water samples with different salt concentrations

The isotopic ratios obtained for the solutions of sea salts are shown in Fig. 5, Table 1 and Table 2. The precision of the $^{18}\text{O}/^{16}\text{O}$ isotopic ratio of the “Nafion membranes” analyses (between 0.056‰ and 0.067‰) was slightly better than for the “automatic injector” analyses (0.091‰). We obtained similar results for the samples containing different matrices (see Section 3.2). However, we did not find any specific trend in the precision for $^2\text{H}/^1\text{H}$ isotopic ratios, which ranged between 0.225‰ and 0.285‰ for both the “automatic injector” and the “Nafion membranes” measurements.

The average absolute difference of the isotopic ratios of the “automatic injector” and the “Nafion membranes” measurements ranged between 1.002‰ and 2.559‰ for $^2\text{H}/^1\text{H}$ and between 0.269‰ and 0.552‰ for $^{18}\text{O}/^{16}\text{O}$ isotopic ratios. The differences were larger for both isotopic ratios when using the medium thickness membrane (N-115), trending generally towards more depleted values. This could be due to the presence of different cations (Na^+ , K^+ , Mg^{2+} , Ca^{2+} , Sr^{2+} ...) and anions (Cl^- , SO_4^{2-} , CO_3^{2-} ...) in the water solutions (other than just H^+ and OH^-), taking into account that the membrane water uptake decreases with the increase of the cation size (lower hydration radius). This, in turn, favours a stronger interaction between cations and the anionic groups in the membrane, decreasing the effective fixed charge concentration [65]. Hence, the membrane capacity for excluding coions (anions) decreases [65]. Smaller differences were found for the thinnest membrane (N-212), since the possibility of the ions for enlarging the internal channels within denser membranes (thinner membranes) is lower, therefore they are less influenced by the ion nature [65]. On the contrary, the concentration of coions in the membrane structure seems to increase with membrane thickness (less dense membranes) [65], which could explain the larger differences of the isotopic ratios obtained with the membrane N-115. As we suggested in Section 3.2, those ions could create a network that hinders the passage through the membrane of the larger atoms, such as the oxygen, resulting in fractionation. There could also be an oxygen exchange between the water and the anions in the structure of the membrane. At the same time, those anions could interact preferentially with the heavy hydrogen isotopes in the membrane structure, explaining the more depleted

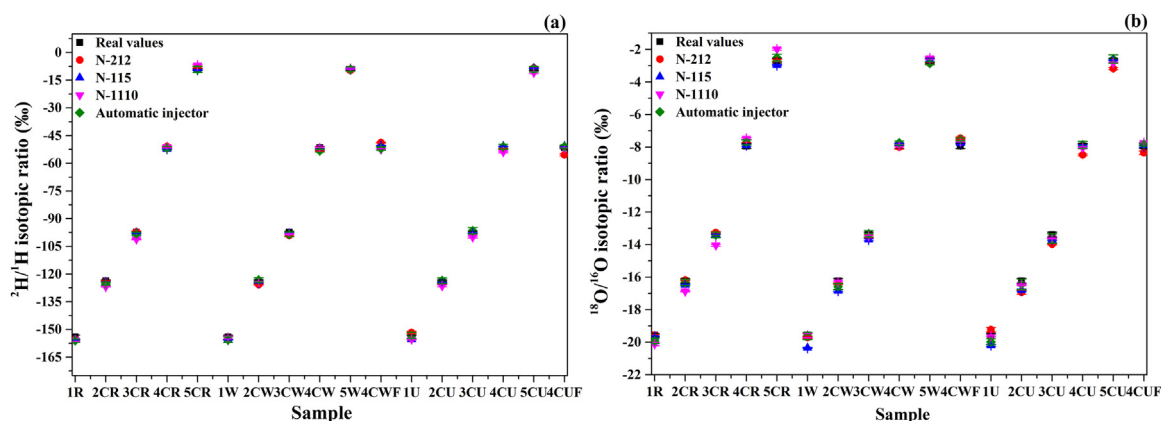


Fig. 4. Isotopic ratios of the samples containing mixtures of five LGR standard waters (1, 2C, 3C, 4C, 5C) and different matrices extracted from the rainfall sample (R), Weierbach streamwater sample (W; WF) and Atter River sample (U; UF), when using three Nafion membranes of different thickness (N-212, N-115, N-1110) and an automatic injector: a) $^2\text{H}/^1\text{H}$ isotopic ratios and b) $^{18}\text{O}/^{16}\text{O}$ isotopic ratios.

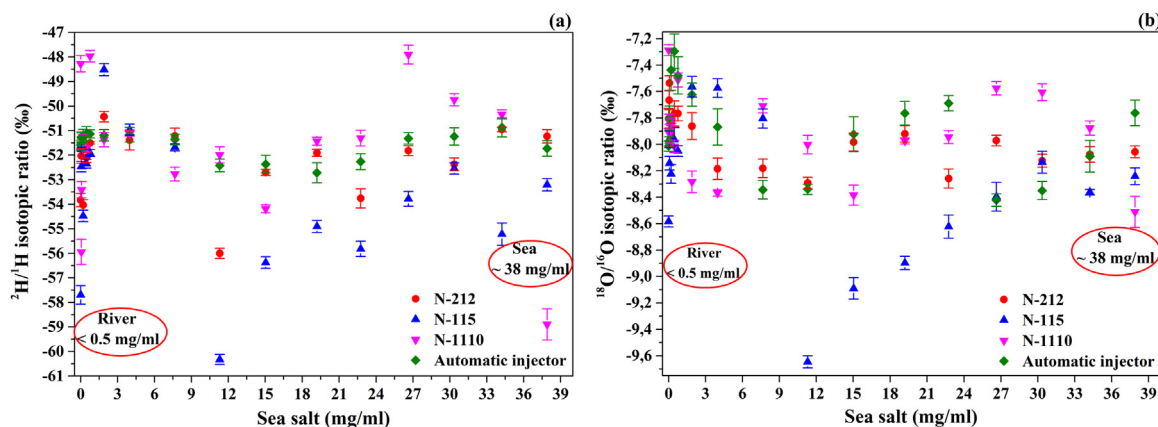


Fig. 5. Isotopic ratios of seventeen solutions with sea salt concentration ranging from 0 to 38 mg/ml covering from the salinity of rivers (< 0.5 mg/ml) to the salinity of sea water (~38 mg/ml) when using three Nafion membranes of different thickness (N-212, N-115, N-1110) and an automatic injector: a) $^2\text{H}/^1\text{H}$ isotopic ratios and b) $^{18}\text{O}/^{16}\text{O}$ isotopic ratios.

results.

On the other hand, the membrane water uptake increases with membrane thickness, probably due to the increase of the ion-exchange capacity and the decrease of the density with thickness. This increases the water transport and hence reduces the average cation transport through the membrane [65]. Therefore, the results obtained when using the thickest membrane (N-1110) end up being close to those obtained when using the thinnest membrane (N-212). The water uptake is indeed large enough to overcome the effect of the larger ions present in the solution. This suggests that the worse accuracy and precision obtained for the $^{18}\text{O}/^{16}\text{O}$ isotopic ratios in the samples containing the Attert River matrix (see Section 3.2) with the thinnest membrane might be more likely due to the interaction of some molecules of pollutants present in the river. They might contain large charged ions, probably more hydrophilic, that are able to enter the structure of the densest membrane, creating fractionation.

Fig. 6 is a zoomed in version of Fig. 5. It shows measurements for the first six samples, which have salinity values ranging from 0 to 0.76 mg/ml. Note that the usual salinity in rivers is below 0.5 mg/ml. Table 1 and Table 2, show no improvement in the precision and the average accuracy of these samples compared to the samples with the higher concentration of salts. Regarding the average absolute difference between the isotopic ratios for the “automatic injector” and the “Nafion membranes” measurements of the samples with low salinity, they show the same trend compared to that found for the samples with higher salinity. Therefore, salinity does not appear to affect the use of the Nafion membranes for the isotopic ratio analysis in water when using

thinner (denser) membranes (N-212, 50.8 μm) or thicker membranes (N-1110, 254 μm).

4. Conclusion

Nafion membranes have been studied as a membrane introduction (MI) inlet system for isotopic ratio measurements in water. They allow directly the conversion of water into water vapour before analysis. Here we studied the potential fractionation of the stable isotopes of the water molecule ($^2\text{H}/^1\text{H}$ and $^{18}\text{O}/^{16}\text{O}$) when passing through Nafion membranes of different thicknesses and under the influence of a wide range of conditions: multiple water matrices, wide salinity range and different isotopic ratios values. Investigated water samples are representative of waters found in the environment. In general, our results show a minor or no influence of neither the matrix (organic matter, pollution), nor water salinity on the measurements for a wide range of isotopic ratios. Nonetheless, we detected that the use of Nafion membranes with a thickness exceeding 150 μm lead to less precise and less accurate measurements. We argued that these results might be associated with the occurrence of fractionation processes. In most cases, the use of the thinnest Nafion membrane (N-212, 50.8 μm) provided the best results. On the contrary, thicker membranes performed better for $^2\text{H}/^1\text{H}$ isotopic ratio when analysing samples containing organic matter, whereas the thicker membranes performed better for $^{18}\text{O}/^{16}\text{O}$ isotopic ratio when the analysing samples are contaminated with pollutants. Thicker membranes are also well suited for both isotopic ratios in water with high salinity, providing similar results to that found for the thinnest

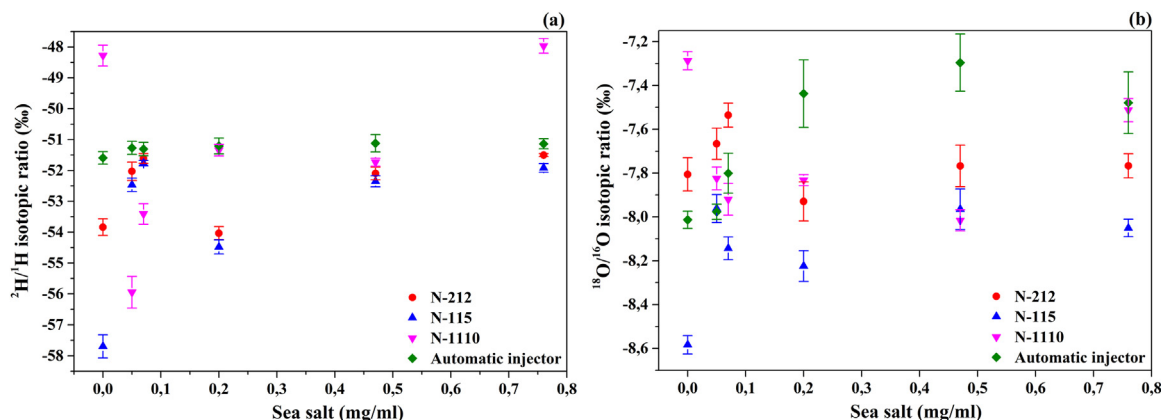


Fig. 6. Isotopic ratios of six solutions with sea salt concentration ranging from 0 to 0.76 mg/ml when using three Nafion membranes of different thickness (N-212, N-115, N-1110) and an automatic injector: a) $^2\text{H}/^1\text{H}$ isotopic ratios and b) $^{18}\text{O}/^{16}\text{O}$ isotopic ratios.

membrane. We linked this to the fact that thicker membranes are more difficult to pass and are more selective to water molecules.

Further studies are, nonetheless, needed to identify which type of pollutants interfered in the $^{18}\text{O}/^{16}\text{O}$ isotopic ratio measurements, as well as the type of organic matter that interfered in the $^2\text{H}/^1\text{H}$ isotopic ratio measurements. Also, the membranes filter the matter suspended in the target samples, improving the precision of the analysis compared to those done with the automatic injector using a conventional filter. Hence, our results show that Nafion membranes are suitable for on-line isotopic ratio monitoring in water, providing a simple, fast and low-cost (no sample collection, transportation, laboratory material, labour) method that avoids sample preparation and reduces energy and time consumption. It could allow the detection of a peak of isotope enrichment or depletion without the presence of an operator. Consequently, Nafion membranes can be linked to either laser-based instruments or mass spectrometer instruments for in-situ analysis of water stable isotopes in the field and at high frequencies. This, in turn, might help to develop portable and field-deployable laser-based and/or mass spectrometer instruments not only to elucidate the fine temporal changes that occur in rapidly responding hydrosystems, but also to develop new applications related to life sciences and geosciences, such as paleoclimatology, forensics, environmental monitoring and ecology.

Acknowledgements

The financial support for this research was provided by the Fonds National de la Recherche Luxembourg (grants FIELDSPEC PoC/13/01 and JEDI INTER-Mobility/15/10948104).

References

- [1] C. Kendall, E.A. Caldwell, Fundamentals of isotope geochemistry, in: C. Kendall, J.J. McDonnell (Eds.), *Isotope Tracers in Catchment Hydrology*, Elsevier Science B.V., Amsterdam, 1998, pp. 51–86.
- [2] M. Küttel, E.J. Steig, Q. Ding, A.J. Monaghan, D.S. Battisti, Seasonal climate information preserved in West Antarctic ice core water isotopes: relationships to temperature, large-scale circulation, and sea ice, *Clim. Dyn.* 39 (2012) 1841–1857.
- [3] B.M. Vinther, P.D. Jones, K.R. Briffa, H.B. Clausen, K.K. Andersen, D. Dahl-Jensen, S.J. Johnsen, Climatic signals in multiple highly resolved stable isotope records from Greenland, *Quat. Sci. Rev.* 29 (2010) 522–538.
- [4] A. Perşoiu, B.P. Onac, J.G. Wynn, A.-V. Bojar, K. Holmgren, Stable isotope behavior during cave ice formation by water freezing in Scărișoara Ice Cave, Romania, *J. Geophys. Res.* 116 (2011) D02111.
- [5] J. Jouzel, R.D. Köster, R.J. Suozzo, G.L. Russell, Stable water isotope behavior during the last glacial maximum: a general circulation model analysis, *J. Geophys. Res.* 99 (1994) 25791–25802.
- [6] S. Nakaya, K. Uesugi, Y. Motodate, I. Ohmiya, H. Komiya, H. Masuda, M. Kusakabe, Spatial separation of groundwater flow paths from a multi-flow system by a simple mixing model using stable isotopes of oxygen and hydrogen as natural tracers, *Water Resour. Res.* 43 (2007) W09404, <https://doi.org/10.1029/2006WR005059>.
- [7] J. González-Trinidad, A. Pacheco-Guerrero, H. Jérez-Ferreira, C. Bautista-Capetillo, A. Hernández-Antonio, Identifying groundwater recharge sites through environmental stable isotopes in an alluvial aquifer, *Water* 9 (2017) 569, <https://doi.org/10.3390/w9080569>.
- [8] B. Nisi, B. Raco, E. Dotsika, Groundwater contamination studies by environmental isotopes: a review, in: A. Scozzari, E. Dotsika (Eds.), *Threats to the Quality of Groundwater Resources. The Handbook of Environmental Chemistry*, 40 Springer, Berlin, Heidelberg, 2014, pp. 115–150.
- [9] O. Kracht, M. Gresch, W. Güjer, Innovative tracer methods for infiltration monitoring, in: *Proceedings of the 10th International Conference on Urban Drainage, Copenhagen/Denmark*, 21–26 August, 2005.
- [10] T.E. Dawson, S. Mambelli, A.H. Plamboeck, P.H. Templer, K.P. Tu, Stable isotopes in plant ecology, *Annu. Rev. Ecol. Syst.* 33 (2002) 507–559.
- [11] Q. Yang, H. Xiao, L. Zhao, M. Zhou, C. Li, S. Cao, Stable isotope techniques in plant water sources: a review, *Sci. Cold Arid Res.* 2 (2) (2010) 0112–0122.
- [12] C. Moreno-Gutiérrez, T.E. Dawson, E. Nicolás, J.I. Querejeta, Isotopes reveal contrasting water use strategies among coexisting plant species in a Mediterranean ecosystem, *New Phytol.* 196 (2012) 489–496.
- [13] P.Z. Ellsworth, D.G. Williams, Hydrogen isotope fractionation during water uptake by woody xerophytes, *Plant Soil* 291 (2007) 93–107.
- [14] D.X. Soto, L.I. Wassenaar, K.A. Hobson, D. Raubenheimer, Stable hydrogen and oxygen isotopes in aquatic food webs are tracers of diet and provenance, *Funct. Ecol.* 27 (2013) 535–543, <https://doi.org/10.1111/1365-2435.12054>.
- [15] J.R. Ehleringer, T.E. Cerling, J.B. West, D.W. Podlesak, L.A. Chesson, G.J. Bowen, Spatial considerations of stable isotope analyses in environmental forensics, in: R.E. Hester, R.M. Harrison (Eds.), *Issues in Environmental Science and Technology* vol. 26, Environmental Forensics, The Royal Society of Chemistry, Cambridge, 2008, pp. 36–53.
- [16] T. Vitvar, P.K. Aggarwal, J.J. McDonnell, A review of isotope applications in catchment hydrology, in: P.K. Aggarwal, J.R. Gat, K.F.O. Froehlich (Eds.), *Isotopes in the Water Cycle: Past, Present and Future of a Developing Science*, Springer, Netherlands, 2005, pp. 151–169, https://doi.org/10.1007/1-4020-3023-1_12.
- [17] J. Klaus, J.J. McDonnell, Hydrograph separation using stable isotopes: review and evaluation, *J. Hydrol.* 505 (2013) 47–64, <https://doi.org/10.1016/j.jhydrol.2013.09.006>.
- [18] H. Craig, Isotope variations in meteoric waters, *Science* 133 (1961) 1702–1703.
- [19] E.S.F. Berman, M. Gupta, C. Gabrielli, T. Garland, J.J. McDonnell, High-frequency field-deployable isotope analyzer for hydrological applications, *Water Resour. Res.* 45 (2009) 1–7, <https://doi.org/10.1029/2009WR008265>.
- [20] L.A. Pangle, J. Klaus, E.S.F. Berman, M. Gupta, J.J. McDonnell, A new multisource and high-frequency approach to measuring $\delta^2\text{H}$ and $\delta^{18}\text{O}$ in hydrological field studies, *Water Resour. Res.* 49 (2013) 7797–7803, <https://doi.org/10.1002/2013WR013743>.
- [21] J. von Freyberg, B. Studer, J. Kirchner, High-frequency isotopic analysis of liquid water samples in the field—initial results from continuous water sampling and cavity ring-down spectroscopy, *Geophys. Res. Abstr.* 18 (2016) (EGU2016-3380-1, EGU General Assembly 2016).
- [22] H. Borsdorf, A. Rämmler, Continuous on-line determination of methyl tert-butyl ether in water samples using ion mobility spectrometry, *J. Chromatogr. A* 1072 (2005) 45–54.
- [23] J.G.A. Devlin, J.A. Amaral, E.T. Krogh, C.G. Gill, A membrane introduction flame ionization/electron capture detection (MIFID/ECD) system for the rapid, real-time screening of volatile disinfection byproducts and hydrocarbon contaminants in water, *Microchem. J.* 88 (2008) 74–81.
- [24] G. Hoch, B. Kok, A mass spectrometer inlet system for sampling gases dissolved in liquid phases, *Arch. Biochem. Biophys.* 101 (1963) 160.
- [25] K.W. Boddeker, Terminology in pervaporation, *J. Membr. Sci.* 51 (1990) 259.
- [26] E.T. Krogh, C.G. Gill, Membrane introduction mass spectrometry (MIMS): a versatile tool for direct, real-time chemical measurements, *J. Mass Spectrom.* 49 (2014) 1205–1213.
- [27] M.A. LaPack, J.C. Tou, C.G. Enke, Membrane mass spectrometry for the direct trace analysis of volatile organic compounds in air and water, *Anal. Chem.* 62 (1990) 1265–1271.
- [28] R.C. Johnson, R.G. Cooks, T.M. Allen, E. Cisper, P.H. Hemberger, Membrane Introduction Mass Spectrometry: trends and applications, *Mass Spectrom. Rev.* 19 (2000) 1–37.
- [29] R.A. Ketola, T. Kotiaho, M.E. Cisper, T.M. Allen, Environmental applications of membrane introduction mass spectrometry, *J. Mass Spectrom.* 37 (2002) 457–476.
- [30] R.T. Short, S.K. Toler, G.P.G. Kibelka, D.T. Rueda Roa, R.J. Bell, R.H. Byrne, Detection and quantification of chemical pesticides using a portable underwater membrane introduction mass spectrometer, *Trends Anal. Chem.* 25 (2006) 637–646.
- [31] C. Janfelt, F.R. Lauritsen, S.K. Toler, R.J. Bell, R.T. Short, Method for quantification of chemicals in a pollution plume using a moving membrane-based sensor exemplified by mass spectrometry, *Anal. Chem.* 79 (2007) 5336–5342.
- [32] J.M. Etzkorn, N.G. Davey, A.J. Thompson, A.S. Creba, C.W. LeBlanc, C.D. Simpsom, E.T. Krogh, C.G. Gill, The use of MIMS-MS-MS in field locations as an on-line quantitative environmental monitoring technique for trace contaminants in air and water, *J. Chromatogr. Sci.* 47 (2009) 57–66.
- [33] B. Brkić, N. France, S. Taylor, Oil-in-water monitoring using membrane inlet mass spectrometry, *Anal. Chem.* 83 (2011) 6230–6236.
- [34] S. Maher, F.P.M. Jjunju, I.S. Young, B. Brkić, S. Taylor, Membrane inlet mass spectrometry for in situ environmental monitoring, *Spectrosc. Eur.* 26 (2014) 6–8.
- [35] T. Aggerholm, F.R. Lauritsen, Direct detection of polyaromatic hydrocarbons, estrogenic compounds and pesticides in water using desorption chemical ionization membrane inlet mass spectrometry, *Rapid Commun. Mass Spectrom.* 15 (2001) 1826–1831.
- [36] H. Frandsen, C. Janfelt, F.R. Lauritsen, Fast and direct screening of polyaromatic hydrocarbon (PAH)-contaminated sand using a miniaturized membrane inlet mass spectrometer (mini-MIMS), *Rapid Commun. Mass Spectrom.* 21 (2007) 1574–1578.
- [37] M. Beckmann, S.K. Sheppard, D. Lloyd, Mass spectrometry monitoring of gas dynamics in peat monoliths: effects of temperature and diurnal cycles on emissions, *Atmos. Environ.* 38 (2004) 6907–6913.
- [38] C.G. Laing, T.G. Shreeve, D.M.E. Pearce, Methane bubbles in surface peat cores: *in situ* measurements, *Glob. Change Biol.* 14 (2008) 916–924.
- [39] S. Giannoukos, B. Brkić, S. Taylor, N. France, Membrane inlet mass spectrometry for homeland security and forensic applications, *J. Am. Soc. Mass Spectrom.* 26 (2014) 231–239.
- [40] S. Church, Del. firm installs fuel cell, *News J.* 6 (2006) B7.
- [41] Q. Zhao, P. Majsztrik, J. Benziger, Diffusion and interfacial transport of water in Nafion, *J. Phys. Chem. B* 115 (2011) 2717–2727.
- [42] T. Takamatsu, M. Hashiyama, A. Eisenberg, Sorption phenomena in Nafion membranes, *J. Appl. Polym. Sci.* 24 (11) (1979) 2199–2220.
- [43] H.L. Yeager, A. Steck, Cation and water diffusion in Nafion ion-exchange membranes—influence of polymer structure, *J. Electrochem. Soc.* 128 (1981) 1880–1884.
- [44] T.A. Zawodzinski, C. Derouin, S. Radzinski, R.J. Sherman, V.T. Smith, T.E. Springer, G. Shimshon, Water uptake by and transport through Nafion® 117 membranes, *J. Electrochem. Soc.* 140 (1993) 1041–1047.
- [45] S. Motupally, A.J. Becker, J.W. Weidner, Diffusion of water in Nafion 115 membranes, *J. Electrochem. Soc.* 147 (9) (2000) 3171–3177.
- [46] S.H. Ge, X.G. Li, B.L. Yi, I.M. Hsing, Absorption, desorption, and transport of water in polymer electrolyte membranes for fuel cells, *J. Electrochem. Soc.* 152 (2005)

- A1149–A1157.
- [47] P.W. Majsztrik, M.B. Satterfield, A.B. Bocarsly, J.B. Benziger, Water sorption, desorption and transport in Nafion membranes, *J. Membr. Sci.* 301 (2007) 93–106.
 - [48] T. Romero, W. Mérida, Water transport in liquid and vapour equilibrated Nafion™ membranes, *J. Membr. Sci.* 338 (2009) 135–144.
 - [49] Q. Duan, H. Wang, J. Benziger, Transport of liquid water through Nafion membranes, *J. Membr. Sci.* 392–393 (2012) 88–94.
 - [50] Y. Li, Q.T. Nguyen, C.L. Buquet, D. Langevin, M. Legras, S. Marais, Water sorption in Nafion® membranes analyzed with an improved dual-mode sorption model-Structure/property relationships, *J. Membr. Sci.* 439 (2013) 1–11.
 - [51] D.K. Kim, E.J. Choi, H.H. Song, M.S. Kim, Experimental and numerical study on the water transport behavior through Nafion® 117 for polymer electrolyte membrane fuel cell, *J. Membr. Sci.* 497 (2016) 194–208.
 - [52] X. Wu, X. Wang, G. He, J. Benziger, Differences in water sorption and proton conductivity between Nafion and SPEEK, *J. Polym. Sci. Part B Polym. Phys.* 49 (2011) 1437–1445.
 - [53] O. Savadogo, Emerging membranes for electrochemical systems Part II. High temperature composite membranes for polymer electrolyte fuel cell (PEFC) applications, *J. Power Sources* 127 (2004) 135–161.
 - [54] S.G. Rinaldo, C.W. Monroe, T. Romero, W. Mérida, M. Eikerling, Vaporization-exchange model for dynamic water sorption in Nafion: transient solution, *Electrochem. Commun.* 13 (2011) 5–7.
 - [55] J. Neel, Introduction to Pervaporation, in: R.Y.M. Huang (Ed.), *Pervaporation Membrane Separation Processes*, 1 Elsevier Science B.V., Amsterdam, 1991, pp. 1–109.
 - [56] V. López-Díaz, H.Q. Hoang, N. Martínez-Carreras, F. Barnich, T. Wirtz, L. Pfister, J. McDonnell, FieldSpec: a field portable mass spectrometer prototype for high frequency measurements of ^2H and ^{18}O ratios in water, *Geophys. Res. Abstr.* 18 (2016) EGU2016- 15573. EGU General Assembly 2016).
 - [57] M.B. Rozenkevich, I.L. Rastunova, O.M. Ivanchuk, S.V. Prokunin, Rate of water transport through MF-4SK sulfocationic membrane, *Russ. J. Phys. Chem.* 77 (6) (2003) 1000–1003.
 - [58] <http://www.lgrinc.com/documents/LGR_IWA%202017-06-29.pdf>.
 - [59] M. Gröning, M. Van Duren, L. Andreescu, Metrological characteristics of the conventional measurement scales for hydrogen and oxygen stable isotope amount ratios: the δ -scales, in: *Combining and Reporting Analytical Results*, A. Fajgelj, M. Belli, U. Sansone (Eds.), *Proceedings of an International Workshop on Combining and reporting analytical results: The role of traceability and uncertainty for comparing analytical results*, Rome, 6–8 March 2006, Royal Society of Chemistry, 2007, pp. 62–72.
 - [60] <<https://www.chemours.com/>>.
 - [61] <<http://www.lgrinc.com/analyzers/isotope/liquid-water-isotope-analyzer>>.
 - [62] D. Penna, B. Stenni, M. Sanda, S. Wrede, T.A. Bogaard, A. Gobbi, M. Borga, B.M.C. Fischer, M. Bonazza, Z. Chárová, On the reproducibility and repeatability of laser absorption spectroscopy measurements for $\delta^2\text{H}$ and $\delta^{18}\text{O}$ isotopic analysis, *Hydrol. Earth Syst. Sci.* 14 (2010) 1551–1566.
 - [63] N. Martínez-Carreras, M.P. Schwab, J. Klaus, C. Hissler, In situ and high frequency monitoring of suspended sediment properties using a spectrophotometric sensor, *Hydrol. Process.* 30 (2016) 3533–3540.
 - [64] M. Onderka, S. Wrede, M. Rodný, L. Pfister, L. Hoffmann, A. Krein, Hydrogeologic and landscape controls of dissolved inorganic nitrogen (DIN) and dissolved silica (DSi) fluxes in heterogeneous catchments, *J. Hydrol.* 450–451 (2012) 36–47.
 - [65] M.A. Izquierdo-Gil, V.M. Barragán, J.P.G. Villaluenga, M.P. Godino, Water uptake and salt transport through Nafion cation-exchange membranes with different thickness, *Chem. Eng. Sci.* 72 (2012) 1–9.